

Assessment of LES techniques for mitigating the Grey Area in DDES models

A. Pont-Vílchez^{*‡}, D. Santos^{*}, F.X. Trias^{*}, A. Duben[†], A. Revell[†] and A. Oliva^{*}

^{*} Heat and Mass Transfer Technological Center
Polytechnical University of Catalonia, Terrassa (Barcelona)

arnau@cttc.upc.edu · danisantos@cttc.upc.edu
xavi@cttc.upc.edu · alistair.revell@manchester.ac.uk
alexey.duben@gmail.com · oliva@cttc.upc.edu

[‡]Corresponding author

Abstract

The slow RANS-LES transition is a well-known shortcoming in hybrid turbulence models such as Delayed-Detached Eddy Simulation (DDES). The present work assesses the feasibility of 2D sensitive LES models for naturally triggering turbulence, rather than using the specifically designed techniques available in the literature. This research has been carried out with *OpenFOAM-v1706*, which has been used for simulating the flow in a Backward-Facing Step configuration. The results have been compared with a DNS data set, showing the good mitigation capabilities of such LES techniques. Nevertheless, other cases should be studied before extracting any relevant conclusion.

Introduction

Accurate numerical simulations are essential for understanding the complex flow physics present in many aeronautical applications. RANS models are commonly used in the industry, as they are cost-effective, but their limitations for predicting complex flow behaviours and providing unsteady data are also well-known. Moreover, the routine use of accurate numerical methodologies such as Large Eddy Simulation (LES) require heavy computational cost, so their applications are not yet feasible. In this regard, Delayed-Detached Eddy Simulation (DDES)⁷ is intended to circumvent the massive costs of pure LES simulations, modelling the boundary layer using RANS and simulating the unsteady flow behaviour with LES at the core. This hybrid turbulence model is widely used due to its user-friendly non-zonal approach and its proved success in several applications. Especially in those situations where RANS applications are unreliable. Apart from that, hybrid turbulence models (in contrast to RANS) can provide high quality transient data, which is completely necessary for simulating complex coupled physics, such as Fluid-Structure Interaction (FSI) and Computational Aeroacoustics (CAA). It is therefore not surprising that during the last decade, these methods have been gaining importance in the aeronautical industry. However, some of their well-known weaknesses are still present. In particular, the slow transition from RANS to LES leads to unphysical results, delaying the flow instabilities in complex zones such as free shear layers. The zone where this issue take place is named Grey Area (GA). In the literature, there are two main strategies for leading this shortcoming². One of them consists on using artificial oscillations in specific areas (zonal approach), whereas the other is based on reducing the subgrid-scale viscosity (Eq. 1), ν_{sgs} , in LES 2D flow regions. The second approach is preferable as it is aligned with the initial non-zonal DES philosophy.

$$\nu_{sgs} = (C_m \Delta)^2 D_{sgs}(\bar{u}) \quad (1)$$

This reduction could be forced by any of the terms present in Eq. 1. The idea of attributing kinematic sensitivity to the Subgrid-Length Scale (SLS) coefficient, Δ , was initially explored by Mockett et al.² ($\tilde{\Delta}_\omega$) and Shur et al.⁶ ($\Delta_{S_{LA}}$). Later we proposed another approach, which was initially developed for LES⁹ (Δ_{lsq}). Surprisingly, even though Δ_{lsq} was initially designed for LES applications, first studies⁴ show how its performance mitigating the GA in DDES was rather promising. It is important noting here that, in contrast to the other specifically designed techniques for mitigating the GA shortcoming, Δ_{lsq} is completely based on a physical and mathematical basis.

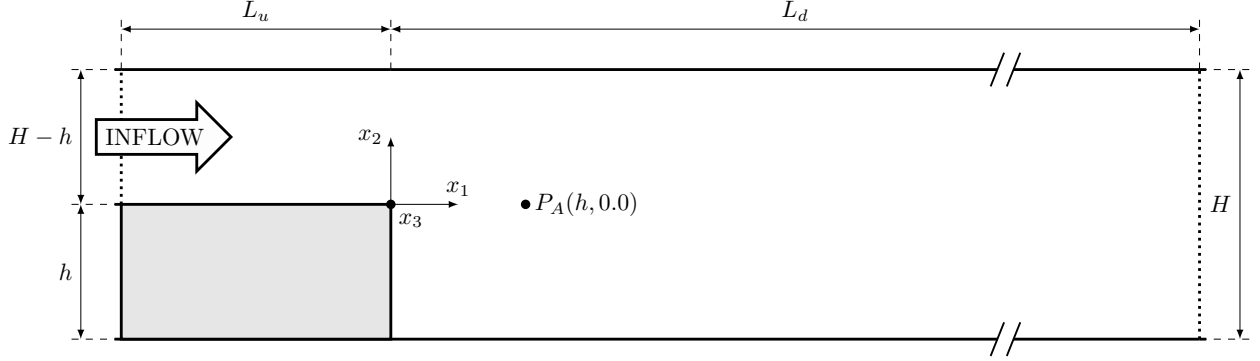


Figure 1: Schematic figure of the Backward Facing Step problem, $ER = H/(H - h) = 2$, and details about its geometry and grid spacing (size of zones and concentration factors; arrows indicate the grid refinement direction). Not to scale.

The significant influence of the differential operator, $D_{sgs}(\bar{u})$, into the GA mitigation was also reported in the literature. Some authors such as Fuchs et al.¹ and Probst et al.⁵ investigated the impact of using the $\sigma - LES$ model, instead of Smagorinsky, due to its ability for switching off in $2D$ flow regions. Taking into account that unsteady $2D$ flows can not be considered as turbulent, the idea of deactivating the model in such regions look reasonable. In fact, the Δ_{SLA} presented by Shur et al.⁶ was also based on the same approach (Eq. 2), as the Δ turned zero in $2D$ flow regions. Therefore, both strategies strengthen the importance of deactivating the turbulence model in $2D$ flow areas.

$$\begin{aligned}
 \nu_{sgs} &= (C_m \Delta_{SLA})^2 D_{sgs}(\bar{u}) \\
 &= (C_m \tilde{\Delta}_\omega)^2 (F_{KH}(\langle VTM \rangle))^2 D_{sgs}(\bar{u}) \\
 &= (C_m \tilde{\Delta}_\omega)^2 D_{sgs}^{2D}(\bar{u}).
 \end{aligned} \tag{2}$$

In this paper, the mitigation capabilities of both strategies, Δ and $D_{sgs}(\bar{u})$, are analysed. The selected configuration case for assessing these methodologies is an incompressible Backward-Facing Step (BFS). The fact that the flow separation is purely induced by geometry, makes this case suitable case for studying the GA numerical issue.

Case Description

Backward-Facing Step represents a canonical configuration to study wall-bounded fluids subjected to sudden expansions (see figure 1). The flow is massively separated at the step-edge, but downstream reattached due to the geometry. The abrupt separation leads to a shear layer, which becomes a source of the well-known Kelvin-Helmholtz instabilities (KH) at high Re values. These instabilities are fed, paired and elongated along the shear layer, affecting the flow behaviour until they impinge at the lower wall. These instabilities are not always well-captured for Hybrid RANS-LES turbulence models due to its slow RANS to LES transition. The fact that the flow separation is purely induced by geometry, makes the BFS a suitable case for studying such numerical issue.

The selected dimensions are $24h \times 2h \times 2h$ in the stream-wise, cross-stream and span-wise direction, respectively. The sudden expansion with an expansion ratio, $ER = H/(H - h)$, equal to 2 is located at $L_u = 4h$ from the inflow. The domain length downstream of the step is $L_d = 20h$. The origin of coordinates is placed at the sharp edge. Regarding the mesh, three different refinement levels at the free shear layer (stream-wise direction downstream the step-edge) have been considered for evaluating the mesh resilience capabilities of the studied strategies. The length of the first node after the step-edge in the stream-wise direction is 8, 16 and 32 times y^+ (inflow conditions). All meshes have 11800 cells per xy -plane and 60 planes in the periodic direction. Concerning the boundary conditions, the inflow is fed with a steady (but turbulent) channel flow profile at $Re_\tau = 395$, which has obtained from a previous RANS simulation. The span-wise and outflow boundary conditions are defined as periodic and convective, respectively. Walls are considered no-slip.

Mathematical Model

The DDES turbulence model presented by Spalart et al.⁷ has been used in this paper, including the Ψ term specially designed to override the unintended low- Re terms. The Hybrid convection scheme presented by Travin et al.⁸ for hybrid $RANS/LES$ calculations is used in this simulation. For the temporal discretisation, a 2^{nd} implicit *backward*

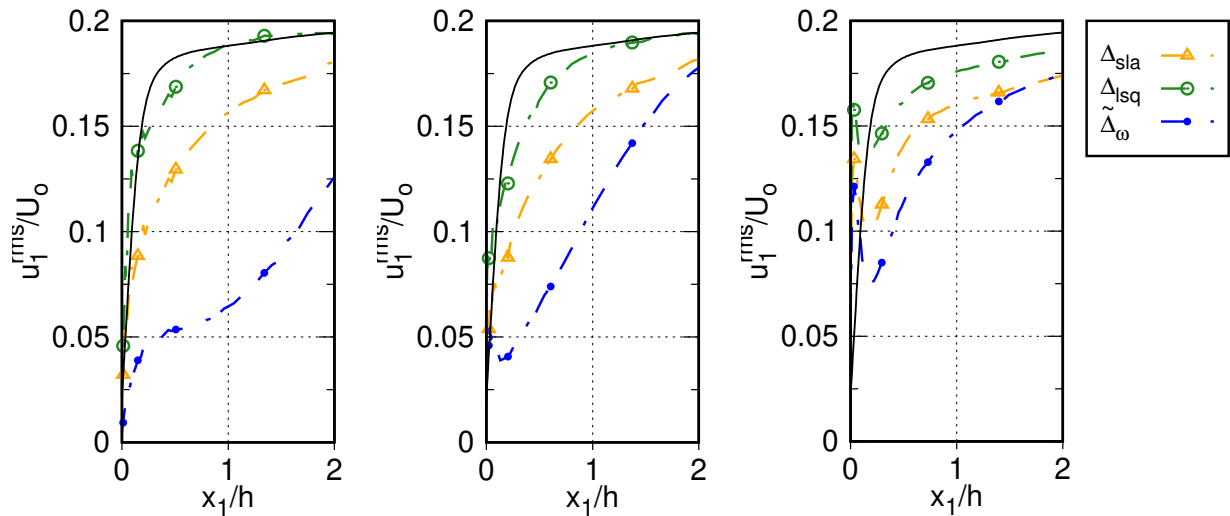


Figure 2: Resolved Reynolds stresses, u_1^{rms} , along the stream-wise direction at $x_2 = 0$, considering similar meshes with different aspect ratios, $\Delta x_1/\Delta x_2$, at the step edge. These are: 8 (left), 16 (middle) and 32 (right). Where U_o refers to the inflow bulk velocity. Reference solid line has been obtained from Pont-Vílchez et al.³

scheme is considered with *Courant* values below 0.8. The velocity-pressure system is coupled using the well-known *PISO* algorithm.

Results

For the sake of clarity, the effect of Δ and $D_{sgs}(\bar{u})$ has been studied separately. The former is focused on the influence of Δ , keeping the LES turbulence model constant (*SMG*). The fact that Δ does not only influence the ν_{sgs} , but also limits the RANS/LES region is a crucial aspect for understanding the observed results. The latter mainly affects the ν_{sgs} value, but also has a significant impact improving the *rms* values at the GA (especially, those differential operators sensitive to *2D* flows).

Subgrid Length Scales, Δ

The influence of the aspect ratio, $\Delta x_1/\Delta x_2$, at the first cell downstream of the step edge is first discussed using the results shown in Fig. 2. For this purpose, three slightly different meshes have been used (see section 2). The highest aspect ratio (right) presents some non-physical oscillations at $x_1/h = 0$. This is not the case for the other two figures (left, centre), where the aspect ratio is considerably smaller. Apart from that, the performance of the SLS in different meshes can also be appreciated. A general good mesh resilience is observed for Δ_{lsq} and Δ_{sla} , whereas $\tilde{\Delta}_\omega$ presents a strong mesh dependency. It can be justified, taking into account that $\tilde{\Delta}_\omega$ strongly depends on the stream-wise cell length in *2D* flow configurations. This is not the case for Δ_{sla} and Δ_{lsq} , as the former is deactivated in *2D* flow areas and the latter mainly depends on the normal cell due to the flow kinematics in such region.⁴ Taking into account the results observed in Fig. 2, from now on the rest of results have been obtained using the mesh with $\Delta x_1/\Delta x_2 = 16$ (middle). The evolution of the mean flow and the *rms* in the stream-wise direction at different positions is shown in figure 3. In this case, we can observe how the mean flow is almost non-affected, whereas the *rms* present only significant differences at the free shear layer zone, where the *GA* shortcoming takes place (Fig. 2).

The effect of the *GA* into the growth of instabilities at the shear layer is also analysed using the same approach described by Pont-Vílchez et al.³ A scheme view of this phenomenon is presented in figure 4 (left). The characteristic length of the instabilities in the stream-wise direction, $\Delta\delta_1$, is calculated using a set of 2-point correlations of u_2' along the stream-wise direction downstream of the step-edge (Fig. 4). Unfortunately, this technique cannot be applied for assessing the size of instabilities in the normal direction, $\Delta\delta_2$, as the flow behaves laminaarly in some parts along the normal direction. For this reason, another approach based on mean quantities has been used,^{3,10}

$$\Delta\delta_2 = \Delta U_1 / (\partial \langle u_1 \rangle / \partial x_2)_{\max}. \quad (3)$$

Even though the *rms* profiles present a strong dependence on the *SLS* (Fig. 2) along the shear layer, this is not so

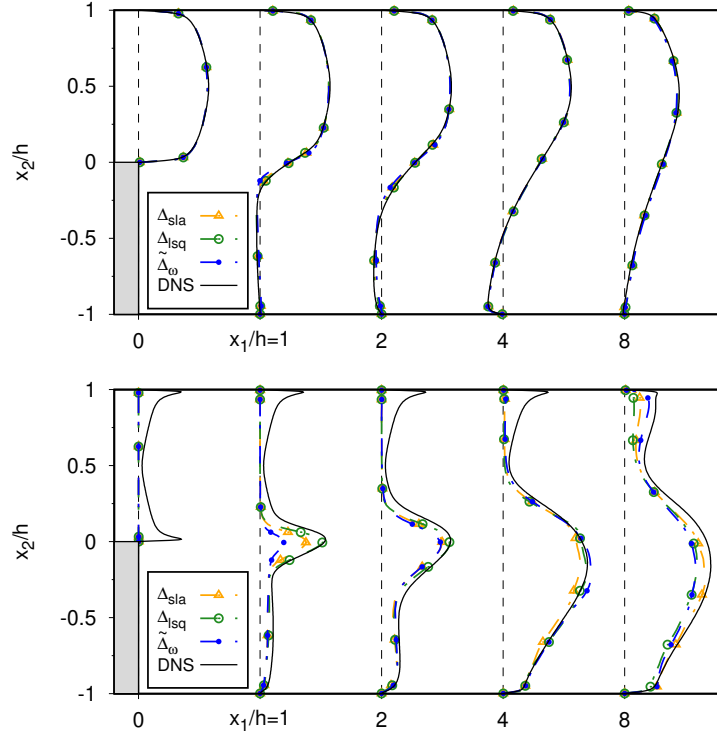


Figure 3: Mean velocity (top), $\langle u_1 \rangle$, and resolved Reynolds stresses (bottom), u_1^{rms} , along the recirculation region downstream the step edge. Reference solid line has been obtained from Pont-Vílchez et al.³

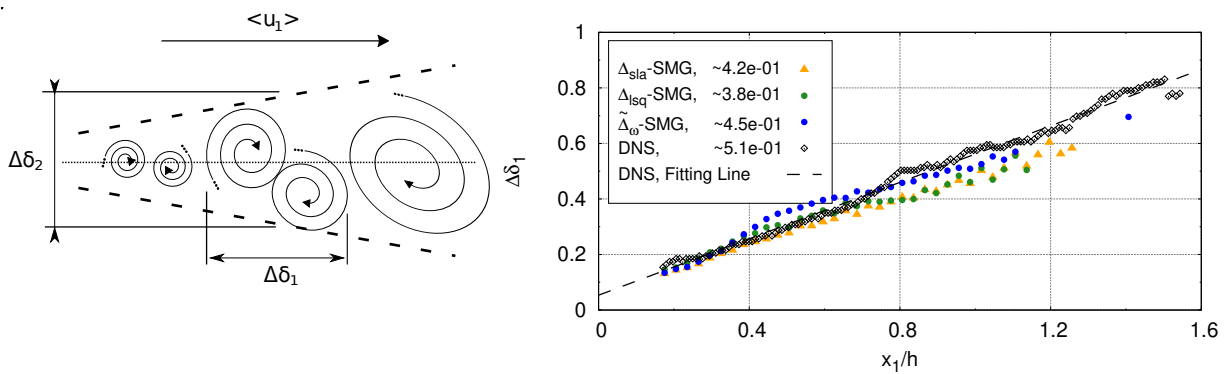


Figure 4: Schematic view of the KH vortices in a shear layer (left) and estimation of the KH rate of growth in the streamwise direction downstream of the step-edge, $\Delta\delta_1$ (right). Different SLS definitions have been used. Reference solid line has been obtained from Pont-Vílchez et al.³

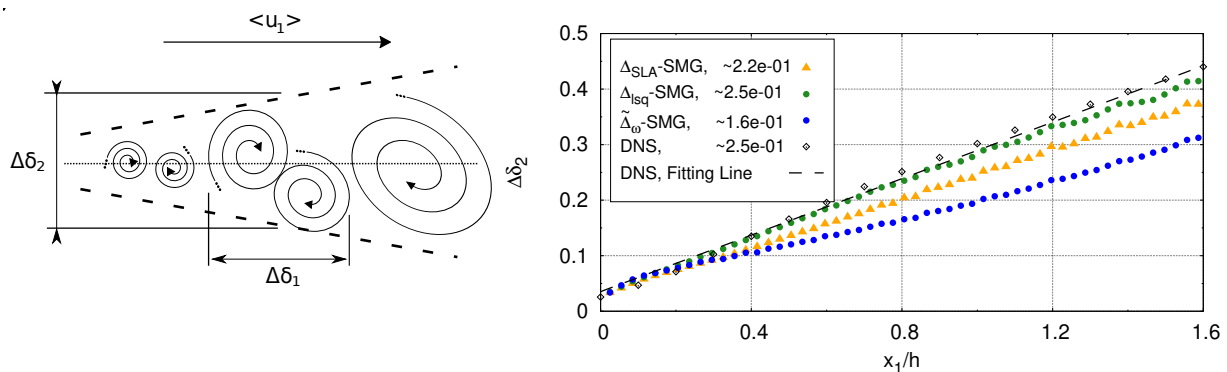


Figure 5: Schematic view of the KH vortices in a shear layer (left) and estimation of the KH rate of growth in the streamwise direction downstream of the step-edge, $\Delta\delta_1$ (right). Different SLS definitions have been used. Reference solid line has been obtained from Pont-Vílchez et al.³

significant in the $\Delta\delta_1$ distribution (Fig.4, right). In particular, Δ_{lsq} , together with Δ_{SLA} , show the best alignment at $x_1 \in [0, 0.7h]$. However, the strength of correlation with DNS data is notably reduced further downstream, leading to a distinct departure of the slope gradient from the reference data, which is mainly attributed to the mesh coarsening in this region. Regarding $\Delta\delta_2$, it seems to be quite sensitive to the SLS (such as *rms* profiles), presenting strong differences in values and slopes (Fig. 5, right). The fact that we are using Eq.3, instead of a 2-point correlation along the normal direction, plays an important role as $(\partial\langle u_1 \rangle / \partial x_2)_{\max}$ is highly influenced by the *rms*. This is clearly observed in figure 5 (right) where the diffusion introduced by Δ_{SLA} and $\tilde{\Delta}_\omega$ may be permitted to grow to excessive levels, preventing the KH instabilities from properly developing along the shear layer.

Differential operator, $D_{sgs}(\bar{u})$

A set of simulations using different operators is presented, including Δ_{SLA} , *SMG*;⁶ $\tilde{\Delta}_\omega$, $\sigma - LES$;¹ $\tilde{\Delta}_\omega$, *S3QR* and Δ_{lsq} , *S3QR*.⁴ In this case all turbulence models are able to be deactivated in free shear layer 2D flow domains, either by Δ_{SLA} or $D_{sgs}^{2D}(\bar{u})$. Different *rms* profiles along the recirculation region are shown in figure 6, as well as the *rms* distribution along the shear layer after the step-edge. Even though a similar positive and linear trend is observed in all cases, the Δ_{lsq} in combination with the *S3QR* provides significantly better results than the other strategies. However, the comparison between the *rms* distribution along the stream-wise direction (bottom) with Fig. 2 (middle) indicates that the *S3QR* turbulence models has a little, if any, contribution to the final result. This is mainly attributed to the predominance of the Δ , which contributes to the definition of the RANS and LES regions. This is not the case for the differential operator, which only affects the ν_{sgs} value in the LES area. Regarding $\tilde{\Delta}_\omega$, both *S3QR* and $\sigma - LES$ improve the mesh resilience capabilities of the SLS (Fig. 2), which is directly observed in figure 6 (bottom). These results are really similar to those provided by Δ_{SLA} , *SMG*, supporting the observations made in section 1. Indeed, the results observed in this section are in good agreement with the studies carried out by Fuchs et al.¹ and Probst et al.,⁵ regarding the importance of using $D_{sgs}(\bar{u})$ sensitive to 2D flows. The growth of the shear layer instabilities along the stream-wise and normal directions is also studied. The former is not shown in this paper, as all simulations exhibit trends similar to those presented in figure 4 (right). The latter is shown in figure 7. In this case, we can observe again the benefits provided by $\sigma - LES$ and *S3QR* in comparison to *SMG*.

Conclusions

This work shows that the use of Δ_{lsq} provides substantial benefits in the free shear layer area respect to the rest of SLS strategies. The influence of differential operators sensitive to 2D is also noticed, especially in combination with those Δ which are sensitive to the stream-wise meshing (such as $\tilde{\Delta}_\omega$). Apparently, the use of such models clearly improves the mesh resilience capabilities of DDES in 2D LES flow regions. The fact that Δ does not only influence the ν_{sgs} , but also defines the RANS/LES regions, explains the significant better results observed by Δ_{lsq} in comparison to the other strategies. Finally, the assessment of the differential operators also show the similarity between the Δ_{SLA} and those $D_{sgs}(\bar{u})$ sensitive to 2D flow regions. While further work is required to investigate whether these observations hold in other flow configurations, these initial results indicate that Δ_{lsq} and $D_{sgs}^{2D}(\bar{u})$ are promising strategies for naturally mitigating the RANS to LES numerical delay.

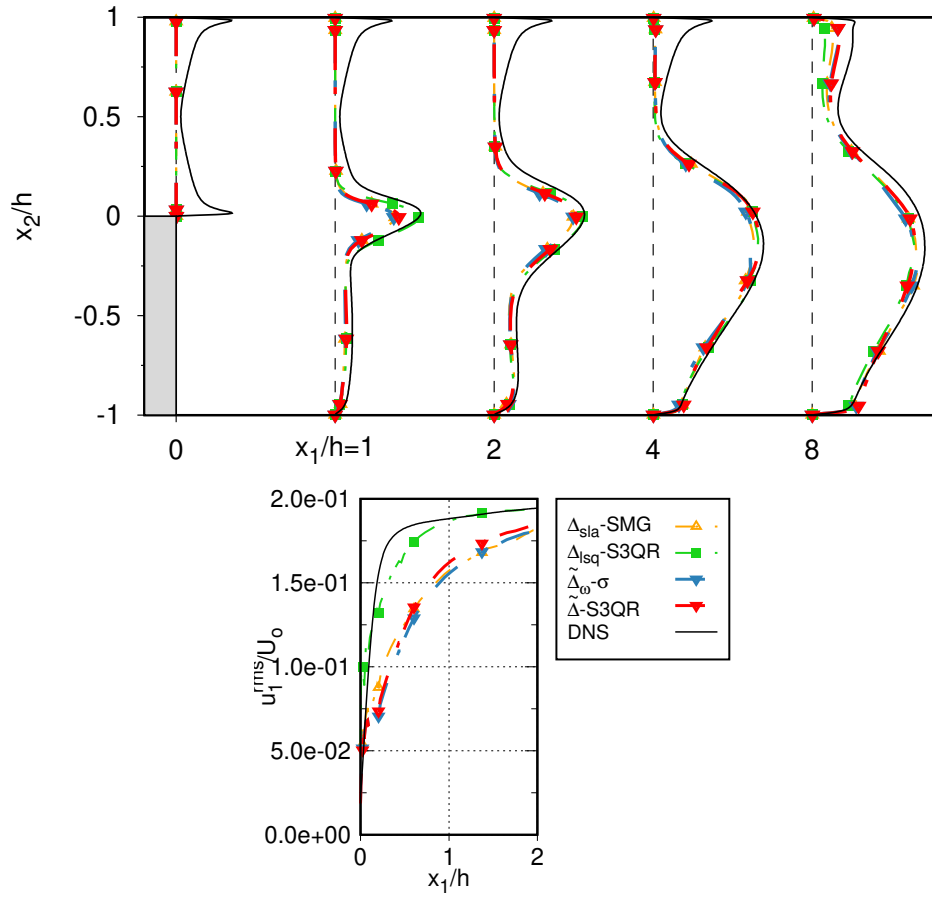


Figure 6: Resolved Reynolds stresses, u_1^{rms} , along the recirculation region downstream the step edge (top) and its evolution in the stream-wise direction (bottom). Reference solid line has been obtained from Pont-Vilchez et al.³

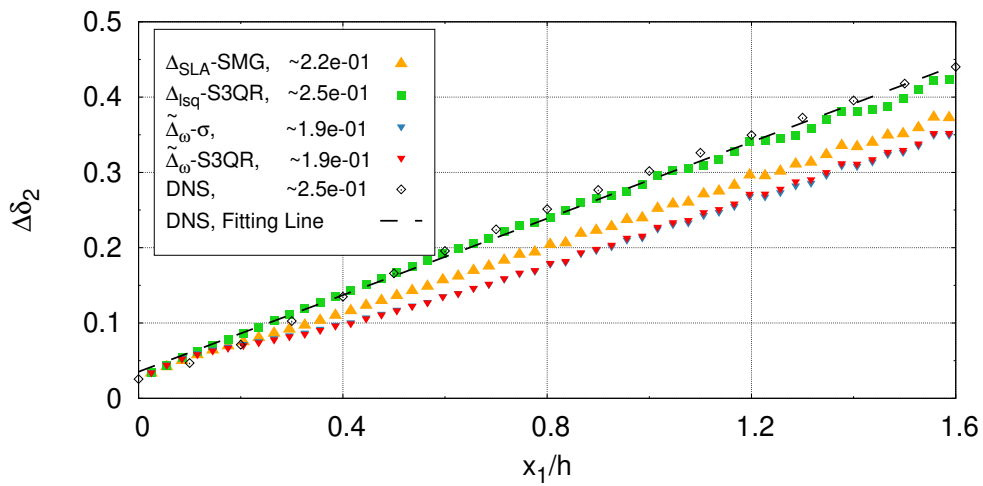


Figure 7: Estimation of the KH rate of growth in the normal direction, $\Delta\delta_2$, downstream of the step-edge using different strategies sensitive to 2D flow regions. Where U_o refers to the inflow bulk velocity.

Acknowledgements

This work has been financially supported by the *Ministerio de Economía y Competitividad*, Spain (No. ENE2017-88697-R). A.P.V. is supported by a *FI-DGR 2016* predoctoral contract (No. 2018FI_B2_00072) financed by *Generalitat de Catalunya*, Spain. F.X.T. is supported by a *Ramón y Cajal* postdoctoral Contract (No. RYC-2012-11996) financed by the *Ministerio de Economía y Competitividad*, Spain.

References

- [1] M. Fuchs, J. Sesterhenn, F. Thiele, and C. Mockett. Assessment of novel DES approach with enhanced SGS modelling for prediction of separated flow over a delta wing. In *22nd AIAA Computational Fluid Dynamics Conference*, 2015.
- [2] Charles Mockett, Marian Fuchs, Andrey Garbaruk, Michael Shur, Philippe Spalart, Michael Strelets, Frank Thiele, and Andrey Travin. Two Non-zonal Approaches to Accelerate RANS to LES Transition of Free Shear Layers in DES. In *Progress in Hybrid RANS-LES Modelling*, pages 187–201, Cham, 2015. Springer International Publishing.
- [3] A. Pont-Vílchez, F. X. Trias, A. Gorobets, and A. Oliva. Direct numerical simulation of backward-facing step flow at $Re_\tau = 395$ and expansion ratio 2. *Journal of Fluid Mechanics*, 863:341–363, 2019.
- [4] A Pont-Vílchez, F X Trias, A Revell, and A Oliva. Assessment and comparison of a recent kinematic sensitive subgrid length scale in Hybrid RANS-LES. In *Proc. of Hybrid RANS-LES Methods 7*, 17-19 September, Berlin, Germany, 2018.
- [5] A. Probst, D. Schwaborn, A. Garbaruk, E. Guseva, M. Shur, M. Strelets, and A. Travin. Evaluation of grey area mitigation tools within zonal and non-zonal RANS-LES approaches in flows with pressure induced separation. *International Journal of Heat and Fluid Flow*, 2017.
- [6] Mikhail L. Shur, Philippe R. Spalart, Mikhail Kh Strelets, and Andrey K. Travin. An Enhanced Version of DES with Rapid Transition from RANS to LES in Separated Flows. *Flow, Turbulence and Combustion*, 95(4), 2015.
- [7] P. R. Spalart, S. Deck, M. L. Shur, K. D. Squires, M. Kh Strelets, and A. Travin. A new version of detached-eddy simulation, resistant to ambiguous grid densities. *Theoretical and Computational Fluid Dynamics*, 20(3):181–195, 2006.
- [8] Philippe Spalart, Michael Shur, Michael Strelets, and Andrey Travin. Sensitivity of Landing-Gear Noise Predictions by Large-Eddy Simulation to Numerics and Resolution. *50th AIAA Aerospace Sciences Meeting including the New Horizons Forum and Aerospace Exposition*, (January):1–20, 2012.
- [9] F X Trias, A. Gorobets, and A. Oliva. A new subgrid characteristic length for large-eddy simulation. *Physics of Fluids*, 115109, 2017.
- [10] C. D. Winant and F. K. Browand. Vortex pairing : The mechanism of turbulent mixing-layer growth at moderate Reynolds number. *Journal of Fluid Mechanics*, 63(2):237–255, 1974.